The Forward-in-Time Upstream Advection Scheme: Extension to Higher Orders

CRAIG J. TREMBACK, JAMES POWELL,* WILLIAM R. COTTON AND ROGER A. PIELKE

Colorado State University, Department of Atmospheric Science, Fort Collins, CO 80523

ABSTRACT

A generalized forward-in-time upstream advective operator following the methodology of Crowley is developed and advective schemes of orders 1 through 10 are tested analytically and numerically. Flux forms of these schemes are also derived with Crowley's methodology. It is shown that these flux forms do not reduce to the advective form with constant velocity and grid spacing for schemes of order 3 and higher and they are not as accurate as the advective form. A new flux form is derived which does reduce to the advective form under the conditions of constant velocity and grid spacing.

The schemes were tested in two dimensions using time splitting. In the rotating cone test, the advective and new flux forms performed identically, while the other flux form had larger dissipation and dispersion errors. In the deformational flow field test, the advective forms were unstable for both time steps tested. The flux forms were less unstable for the higher Courant number and the domain as a whole was stable for the lower Courant number.

With respect to order of the various forms, the schemes performed consistent with the linear stability analysis; errors decrease as the order of the scheme becomes greater. The sixth-order schemes appear to be the best balance between efficiency and accuracy.

1. Introduction

Various forms of the forward-in-time, upstream advection scheme have been used and referenced frequently over the past two decades. Examples of such schemes are the classical first-order forward upstream scheme (analyzed by Molenkamp, 1968), the second-order Crowley (1968) scheme and the fourth-order Crowley (1968) scheme. The second-order Crowley scheme has probably received the most attention; researchers have studied its behavior in multiple dimensions (Smolarkiewicz, 1982) and added third-order spatial correction terms (Schlesinger, 1985). It has been used in simulations of almost all scales of atmospheric motion including two-dimensional cloud simulations (Orville and Kopp, 1977; Chen and Orville, 1980).

We will use and expand Crowley's (1968) methodology to upstream schemes of order greater than 4. When we refer to the order of a scheme, we mean the order of spatial accuracy. If the schemes were to be expanded in a Taylor series, the order of the first truncated spatial term would be one larger than the order of the scheme. Thus, a fourth-order scheme has fifth-order errors (order of Δx^5). Similarly, when we refer to the order of accuracy of a scheme, we are referring to the highest-order term that is explicitly included in the scheme. The leading term in the truncation error would

* Current affiliation: Department of Mathematics, University of Arizona, Tucson, AZ 85721.

be one order higher. The number of data points required to produce an nth order scheme is $n + 1$; a fourth-order scheme requires five points of data. Flux-conservative forms of the advection schemes, the effects of constant and variable grid spacing, and the application of these schemes in more than one dimension will be discussed. We will detail the construction of both flux and advective forms and test these schemes analytically and numerically. We will also provide an indication of the relative computational cost of the schemes.

2. The one-dimensional linear upstream advection scheme—derivation and stability

To derive the advection schemes, we will follow the methodology of polynomial fitting, although, as mentioned by Crowley (1968), the same results can be achieved through Taylor series expansions. Our approach is to fit a Lagrangian polynomial of arbitrary degree to a discrete set of data points. This polynomial will be used to predict the value of the data field at a future time level through interpolation. Let U be the advecting velocity and Δt the time step. Intuitively, the value of the polynomial at a distance $U\Delta t$ upwind of the predictive point, x_j, will be that point's value at the next time step. The set of data points used for the polynomial is determined by whether the polynomial is odd or even ordered. For a polynomial of order $2n$, n points will be upwind and another n points downwind of x_j. For a polynomial of $2n + 1$ degree, the extra

point will be added in the upwind direction $(n + 1$ points upwind of x_j). Although any other combination of upwind and downwind points is possible, this set produces the most accurate results for an advection scheme.

The Lagrangian polynomial is

$$P(x, \phi_j^n) = \sum_{k=0}^{ORD} \left[\prod_{m=0, m \neq k}^{ORD} \frac{x - x_m}{x_k - x_m} \right] \phi_k^n \qquad (1)$$

where ORD is the order of the polynomial, ϕ denotes values of the field to be advected and the superscript n designates the time level. Indices k and m vary through the ORD + 1 grid points used for the polynomial. To derive the advection scheme, we will interpolate upstream along P a distance of $U\Delta t$. The advection scheme then becomes

$$\phi_j^{n+1} = P[x_j - U\Delta t, \phi_j^n]. \qquad (2)$$

It is possible to obtain the coefficients of the Lagrangian polynomial using Taylor series expansions. We want to express ϕ^{n+1} as a linear combination of ϕ^n, i.e.,

$$\phi_j^{n+1} = \sum_i a_i \phi_{j+i}^n \qquad (3)$$

where a_i are constants depending on grid spacing, and $i = 0, \pm1, \pm2, \cdots$. Considering the ϕ_{j+i} as samples from a continuous data field ϕ and Δx as a constant grid increment $(x_{j+1} - x_j)$, expanding (3) in a Taylor series gives

$$\sum_{k=0}^{\infty} \frac{(\Delta t)^k}{k!} \frac{\partial^k \phi}{\partial t^k} = \sum_i a_i \left[\sum_{k=0}^{\infty} \frac{(\Delta x)^k}{k!} \frac{\partial^k \phi}{\partial x^k} \right]. \qquad (4)$$

Reorganizing (4) gives

$$\phi_j^n \left(1 - \sum_i a_i\right) + \sum_{k=1}^{\infty} \frac{1}{k!} \left[(\Delta t)^k \frac{\partial^k \phi}{\partial t^k} - \sum_i a_i (\Delta x)^k \frac{\partial^k \phi}{\partial x^k} \right] = 0. \qquad (5)$$

Using

$$\frac{\partial}{\partial t}(\phi) = -U \frac{\partial}{\partial x}(\phi)$$

and assuming U constant gives

$$\frac{\partial^k \phi}{\partial t^k} = (-U)^k \frac{\partial^k \phi}{\partial x^k}.$$

Consequently we have a set of equations

$$\sum_i (x_i - x_j)^k a_i = (-U\Delta t)^k.$$

To obtain the coefficients a_i in (3) for an upstream approximation, restrict i to the same set of points used for the polynomial P and k to 0, 1, . . . , ORD. Solving this system of ORD + 1 equations in ORD + 1 unknowns yields the same expression for ϕ^{n+1} as (2), as demonstrated by Young and Gregory (1972).

The approximation for ϕ_j^{n+1} given by (2) is ORD-order accurate in time and space if the velocity field is uniform; by construction, all truncation errors of order up to and including ORD are zero. However, if the velocity field varies in time or space, as shown by Crowley (1968), these schemes are only first-order accurate in time. The leading terms of the truncation error are of order Δt^2 and are a function of the temporal and spatial gradients of the velocity field.

With Δx constant, each $(x_j - x_m)$ becomes $(j - m)\Delta x$ and x can be expressed in terms of Δx. The advection schemes for values of ORD from 1 through 6, where $\alpha = U\Delta t/\Delta x$, are

ORD = 1 (Forward-upstream):

$$\phi_j^{n+1} = \phi_j^n + \alpha(\phi_{j-1} - \phi_j)$$

ORD = 2 (second-order Crowley):

$$\phi_j^{n+1} = \phi_j^n + \frac{\alpha}{2}(\phi_{j-1} - \phi_{j+1})$$
$$+ \frac{\alpha^2}{2}(\phi_{j-1} - 2\phi_j + \phi_{j+1})$$

ORD = 3:

$$\phi_j^{n+1} = \phi_j^n + \frac{\alpha}{6}(-\phi_{j-2} + 6\phi_{j-1} - 3\phi_j - 2\phi_{j+1})$$
$$+ \frac{\alpha^2}{2}(\phi_{j-1} - 2\phi_j + \phi_{j+1})$$
$$+ \frac{\alpha^3}{6}(\phi_{j-2} - 3\phi_{j-1} + 3\phi_j - \phi_{j+1})$$

ORD = 4 (fourth-order Crowley):

$$\phi_j^{n+1} = \phi_j^n + \frac{\alpha}{12}(-\phi_{j-2} + 8\phi_{j-1} - 8\phi_{j+1} + \phi_{j+2})$$
$$+ \frac{\alpha^2}{24}(-\phi_{j-2} + 16\phi_{j-1} - 30\phi_{j-1}$$
$$+ 16\phi_{j+1} - \phi_{j+2})$$
$$+ \frac{\alpha^3}{12}(\phi_{j-2} - 2\phi_{j-1} + 2\phi_{j+1} - \phi_{j-2})$$
$$+ \frac{\alpha^4}{24}(\phi_{j-2} - 4\phi_{j-1} + 6\phi_j - 4\phi_{j+1} + \phi_{j+2})$$

ORD = 5:

$$\phi_j^{n+1} = \phi_j^n + \frac{\alpha}{60}(2\phi_{j-3} - 15\phi_{j-2} + 60\phi_{j-1} - 20\phi_j$$
$$- 30\phi_{j+1} + 30_{j+2})$$
$$+ \frac{\alpha^2}{24}(-\phi_{j-2} + 16\phi_{j-1} - 30\phi_j + 16\phi_{j+1} - \phi_{j+2})$$
$$+ \frac{\alpha^3}{24}(-\phi_{j-3} + 7\phi_{j-2} - 14\phi_{j-1} + 10\phi_j$$
$$- \phi_{j+1} - \phi_{j+2})$$

$$+\frac{\alpha^4}{24}(\phi_{j-2} - 4\phi_{j-1} + 6\phi_j - 4\phi_{j+1} + \phi_{j-2})$$

$$+\frac{\alpha^5}{120}(\phi_{j-3} - 5\phi_{j-2} + 10\phi_{j-1} - 10\phi_j$$

$$+ 5\phi_{j+1} - \phi_{j+2})$$

ORD = 6:

$$\phi_j^{n+1} = \phi_j^n + \frac{\alpha}{60}(\phi_{j-3} - 9\phi_{j-2} + 45\phi_{j-1}$$

$$- 45\phi_{j+1} + 9\phi_{j+2} - \phi_{j+3})$$

$$+\frac{\alpha^2}{360}(2\phi_{j-3} - 27\phi_{j-2} + 270\phi_{j-1}$$

$$- 490\phi_j + 270\phi_{j+1} - 27\phi_{j+2} + 2\phi_{j+3})$$

$$+\frac{\alpha^3}{48}(-\phi_{j-3} + 8\phi_{j-2} - 13\phi_{j-1}$$

$$+ 13\phi_{j+1} - 8\phi_{j+2} + \phi_{j+3})$$

$$+\frac{\alpha^4}{144}(-\phi_{j-3} + 12\phi_{j-2} - 39\phi_{j-1}$$

$$+ 56\phi_j - 39\phi_{j+1} + 12\phi_{j+2} - \phi_{j+3})$$

$$+\frac{\alpha^5}{240}(\phi_{j-3} - 4\phi_{j-2} + 5\phi_{j-1} - 5\phi_{j+1}$$

$$+ 4\phi_{j+2} - \phi_{j+3})$$

$$+\frac{\alpha^6}{720}(\phi_{j-3} - 6\phi_{j-2} + 15\phi_{j-1} - 20\phi_j$$

$$+ 15\phi_{j+1} - 6\phi_{j+2} + \phi_{j+3}).$$

The schemes of orders 7 through 10 are given in the Appendix. The third-order scheme has also been discussed by Takacs (1985).

A standard von Neumann stability analysis was performed on the ten schemes. The results, presented in Tables 1 and 2, suggest

- Even-ordered terms most affect amplitude errors and odd-ordered terms are most responsible for phase errors. An even-order scheme decreases the amplitude error of the next lower-order odd scheme, but phase errors are slightly increased. Conversely, an odd-order scheme will improve phase accuracy but increase amplitude errors over the next lower-order even scheme.
- As the order of the scheme increases, the rate of improvement decreases. The sixth-order scheme is probably the best balance between complexity and accuracy.
- All schemes have the Courant–Friedrich–Levy stability criterion, $\alpha \leqslant 1$.
- Odd schemes have more damping than even schemes. Odd-order schemes also cost more to execute

TABLE 1. Amplification factor for the advective form and constant grid flux form.

Order	Courant number						
	0.01	0.1	0.3	0.5	0.7	0.9	1.0
	2Δx						
1	0.980	0.800	0.400	0.000	0.400	0.800	1.000
2	1.000	0.980	0.820	0.500	0.020	0.620	1.000
3	0.986	0.848	0.456	0.000	0.456	0.848	1.000
4	1.000	0.973	0.765	0.375	0.147	0.723	1.000
5	0.989	0.868	0.481	0.000	0.481	0.868	1.000
6	1.000	0.970	0.737	0.313	0.225	0.766	1.000
7	0.991	0.880	0.495	0.000	0.495	0.880	1.000
8	1.000	0.968	0.719	0.273	0.272	0.792	1.000
9	0.992	0.888	0.505	0.000	0.505	0.888	1.000
10	1.000	0.966	0.706	0.246	0.305	0.809	1.000
	4Δx						
1	0.990	0.906	0.762	0.707	0.762	0.906	1.000
2	1.000	0.995	0.958	0.901	0.866	0.920	1.000
3	0.997	0.966	0.908	0.884	0.908	0.966	1.000
4	1.000	0.997	0.978	0.952	0.943	0.971	1.000
5	0.999	0.986	0.961	0.950	0.961	0.986	1.000
6	1.000	0.999	0.989	0.978	0.975	0.988	1.000
7	0.999	0.994	0.983	0.978	0.983	0.994	1.000
8	1.000	0.999	0.995	0.990	0.989	0.995	1.000
9	1.000	0.997	0.992	0.989	0.992	0.997	1.000
10	1.000	1.000	0.998	0.995	0.995	0.998	1.000
	8Δx						
1	0.997	0.973	0.936	0.924	0.936	0.973	1.000
2	1.000	1.000	0.996	0.992	0.989	0.993	1.000
3	1.000	0.997	0.993	0.992	0.993	0.997	1.000
4	1.000	1.000	1.000	0.999	0.999	0.999	1.000
5	1.000	1.000	0.999	0.999	0.999	0.999	1.000
6	1.000	1.000	1.000	1.000	1.000	1.000	1.000
7	1.000	1.000	1.000	1.000	1.000	1.000	1.000
8	1.000	1.000	1.000	1.000	1.000	1.000	1.000
9	1.000	1.000	1.000	1.000	1.000	1.000	1.000
10	1.000	1.000	1.000	1.000	1.000	1.000	1.000

efficiently on a vector-based computer; the asymmetry of the odd scheme (one extra upwind point) requires a decision regarding upwind direction or the calculation of the advection scheme in both positive and negative velocity directions. These two facts make even-ordered schemes more attractive in most applications.

3. The flux conservative form—derivation and stability

Again following the polynomial fit methodology used by Crowley (1968), a flux conservative form of the ten orders of advective schemes can be derived. The flux form of the one-dimensional advection equation, assuming negligible divergence, is

$$\frac{\partial \phi}{\partial t} = -\frac{\partial u\phi}{\partial x}.$$

In finite difference form

$$\phi_j^{n+1} = \phi_j^n + \frac{\Delta t}{\Delta x}[F_{j+1/2} - F_{j-1/2}]. \tag{6}$$

TABLE 2. Phase speed ratio for the advective form and constant grid flux form.

Order	Courant number						
	0.01	0.1	0.3	0.5	0.7	0.9	1.0
	$4\Delta x$						
1	0.643	0.704	0.859	1.000	1.060	1.033	1.000
2	0.637	0.641	0.676	0.749	0.856	0.964	1.000
3	0.852	0.879	0.945	1.000	1.023	1.013	1.000
4	0.849	0.852	0.873	0.911	0.956	0.991	1.000
5	0.935	0.947	0.976	1.000	1.010	1.006	1.000
6	0.934	0.935	0.946	0.964	0.983	0.997	1.000
7	0.971	0.976	0.989	1.000	1.005	1.003	1.000
8	0.970	0.971	0:976	0.984	0.993	0.999	1.000
9	0.986	0.989	0.995	1.000	1.002	1.001	1.000
10	0.986	0.987	0.989	0.993	0.997	1.000	1.000
	$8\Delta x$						
1	0.903	0.926	0.970	1.000	1.013	1.008	1.000
2	0.900	0.901	0.910	0.928	0.953	0.984	1.000
3	0.989	0.991	0.996	1.000	1.002	1.000	1.000
4	0.988	0.988	0.990	0.992	0.995	0.999	1.000
5	0.999	0.999	1.000	1.000	1.000	1.000	1.000
6	0.999	0.999	0.999	0.999	0.999	1.000	1.000
7	1.000	1.000	1.000	1.000	1.000	1.000	1.000
8	1.000	1.000	1.000	1.000	1.000	1.000	1.000
9	1.000	1.000	1.000	1.000	1.000	1.000	1.000
10	1.000	1.000	1.000	1.000	1.000	1.000	1.000

To derive the flux, $F_{j+1/2}$, the Lagrangian polynomial (1) of one order less than the desired order of the flux scheme is fitted to the points surrounding $x_{j+1/2}$. These points are centered about $x_{j+1/2}$ for odd numbered polynomials and an extra point in the upwind direction is added for even ordered polynomials. The polynomial, $P(x_j, \phi^n)$, is then integrated from $x_{j+1/2} - u\Delta t$ to $x_{j+1/2}$ to arrive at the total flux through a boundary during a time step, i.e.,

$$F_{j+1/2} = \frac{1}{\Delta t} \int_{x_{j+1/2} - u\Delta t}^{x_{j+1/2}} P[x, \phi_j{}^n] dx. \qquad (7)$$

The resulting expressions for fluxes of order 1 through 6, with Δx constant, are

ORD = 1:

$$F_{j+1/2} \frac{\Delta t}{\Delta x} = -\alpha \phi_j$$

ORD = 2:

$$F_{j+1/2} \frac{\Delta t}{\Delta x} = \alpha/2(-\phi_j - \phi_{j+1})$$
$$+ \alpha^2/2(-\phi_j + \phi_{j+1})$$

ORD = 3:

$$F_{j+1/2} \frac{\Delta t}{\Delta x} = \alpha/8(\phi_{j-1} - 6\phi_j - 3\phi_{j+1})$$
$$+ \alpha^2/2(-\phi_j + \phi_{j+1})$$
$$+ \alpha^3/6(-\phi_{j-1} + 2\phi_j - \phi_{j+1})$$

ORD = 4:

$$F_{j+1/2} \frac{\Delta t}{\Delta x} = \alpha/16(\phi_{j-1} - 9\phi_j - 9\phi_{j+1} + \phi_{j+2})$$
$$+ \alpha^2/48(\phi_{j-1} - 27\phi_j + 27\phi_{j+1} - \phi_{j+2})$$
$$+ \alpha^3/12(-\phi_{j-1} + \phi_j + \phi_{j+1} - \phi_{j+2})$$
$$+ \alpha^4/24(-\phi_{j-1} + 3\phi_j - 3\phi_{j+1} + \phi_{j+2})$$

ORD = 5:

$$F_{j+1/2} \frac{\Delta t}{\Delta x} = \alpha/128(-3\phi_{j-2} + 20\phi_{j-1} - 90\phi_j$$
$$- 60\phi_{j+1} + 5\phi_{j+2})$$
$$+ \alpha^2/48(\phi_{j-1} - 27\phi_j + 27\phi_{j+1} - \phi_{j+2})$$
$$+ \alpha^3/144(5\phi_{j-2} - 32\phi_{j-1} + 42\phi_j$$
$$- 8\phi_{j+1} - 7\phi_{j+2})$$
$$+ \alpha^4/24(-\phi_{j-1} + 3\phi_j - 3\phi_{j+1} + \phi_{j+2})$$
$$+ \alpha^5/120(-\phi_{j-2} + 4\phi_{j-1} - 6\phi_j$$
$$+ 4\phi_{j+1} - \phi_{j+2})$$

ORD = 6:

$$F_{j+1/2} \frac{\Delta t}{\Delta x} = \alpha/256(-3\phi_{j-2} + 25\phi_{j-1} - 150\phi_j$$
$$- 150\phi_{j+1} + 25\phi_{j+2} - 3\phi_{j+3})$$
$$+ \alpha^2/3840(-9\phi_{j-2} + 125\phi_{j-1} - 2250\phi_j$$
$$+ 2250\phi_{j+1} - 125\phi_{j+2} + 9\phi_{j+3})$$
$$+ \alpha^3/288(5\phi_{j-2} - 39\phi_{j-1} + 34\phi_j$$
$$+ 34\phi_{j+1} - 39\phi_{j+2} + 5\phi_{j+3})$$
$$+ \alpha^4/192(\phi_{j-2} - 13\phi_{j-1} + 34\phi_j - 34\phi_{j+1}$$
$$+ 13\phi_{j+2} - \phi_{j+3})$$
$$+ \alpha^5/240(-\phi_{j-2} + 3\phi_{j-1} - 2\phi_j - 2\phi_{j+1}$$
$$+ 3\phi_{j+2} - \phi_{j+3})$$
$$+ \alpha^6/720(-\phi_{j-2} + 5\phi_{j-1} - 10\phi_j + 10\phi_{j+1}$$
$$- 5\phi_{j+2} + \phi_{j+3}).$$

Fluxes of order 7 through 10 are given in the Appendix.

Derivation of flux expressions for variable grid spacing is straightforward with this methodology. However, when u and Δx are constant, the flux form (7) does not reduce to the advective form for schemes of order 3 and higher. This can be seen from the definition of the Lagrangian polynomial (1). The advective form involves an interaction of grid spacings between all ORD + 1 points, while the flux form, by integrating a poly-

TABLE 3. Amplification factor for the integrated flux form.

Order	Courant number						
	0.01	0.1	0.3	0.5	0.7	0.9	1.0
$2\Delta x$							
1	0.980	0.800	0.400	0.000	0.400	0.800	1.000
2	1.000	0.980	0.820	0.500	0.020	0.620	1.000
3	0.990	0.881	0.556	0.167	0.223	0.548	0.667
4	0.980	0.786	0.317	0.125	0.462	0.643	0.667
5	0.992	0.903	0.600	0.214	0.172	0.475	0.572
6	0.985	0.830	0.415	0.013	0.357	0.547	0.572
7	0.994	0.914	0.622	0.238	0.146	0.437	0.524
8	0.987	0.853	0.466	0.047	0.302	0.498	0.524
9	0.994	0.921	0.636	0.254	0.129	0.414	0.493
10	0.989	0.867	0.499	0.085	0.267	0.467	0.493
$4\Delta x$							
1	0.990	0.906	0.762	0.707	0.762	0.906	1.000
2	1.000	0.995	0.958	0.901	0.866	0.920	1.000
3	0.997	0.973	0.920	0.886	0.883	0.906	0.920
4	0.998	0.977	0.945	0.935	0.935	0.929	0.920
5	0.999	0.989	0.962	0.938	0.922	0.914	0.910
6	0.999	0.990	0.972	0.957	0.942	0.923	0.910
7	1.000	0.995	0.978	0.958	0.938	0.918	0.907
8	1.000	0.995	0.982	0.966	0.946	0.921	0.907
9	1.000	0.997	0.985	0.966	0.944	0.920	0.906
10	1.000	0.997	0.987	0.970	0.948	0.921	0.906
$8\Delta x$							
1	0.997	0.973	0.936	0.924	0.936	0.973	1.000
2	1.000	1.000	0.996	0.992	0.989	0.993	1.000
3	1.000	0.998	0.994	0.992	0.991	0.992	0.993
4	1.000	0.999	0.998	0.997	0.996	0.994	0.993
5	1.000	1.000	0.999	0.997	0.996	0.994	0.993
6	1.000	1.000	0.999	0.998	0.996	0.994	0.993
7	1.000	1.000	0.999	0.998	0.996	0.994	0.993
8	1.000	1.000	0.999	0.998	0.996	0.994	0.993
9	1.000	1.000	0.999	0.998	0.996	0.994	0.993
10	1.000	1.000	0.999	0.998	0.996	0.994	0.993

where $m = -\mathrm{UP}, -\mathrm{UP} + 1, \cdots, \mathrm{ORD} - \mathrm{UP} - 1$ and UP is the number of points upwind of j in the advective form. Rewriting (6) and using (3),

$$\phi_j^{n+1} = \phi_j^n + \sum_i a_i \phi_{j+i}^n$$

$$= \phi_j^n + \frac{\Delta t}{\Delta x}\left[\sum_m b_m \phi_{j+1+m}^n - \sum_m b_m \phi_{j+m}^n\right] \quad (8)$$

where we have separated ϕ_j^n from (3) and $i = -\mathrm{UP}, -\mathrm{UP} + 1, \cdots, \mathrm{ORD} - \mathrm{UP}$. From (8), by equating similar ϕ_{j+i}, we can find the coefficients b,

$$b_{-\mathrm{UP}} = a_{-\mathrm{UP}} \frac{\Delta x}{\Delta t}$$

$$b_{\mathrm{ORD-UP}-1} = a_{\mathrm{ORD-UP}} \frac{\Delta x}{\Delta t}$$

$$b_m = a_m \frac{\Delta x}{\Delta t} + b_{m-1}.$$

The expressions for constant grid fluxes $F_{j+1/2}$ for orders 1 through 6 are then

ORD = 1:

$$F_{j+1/2} \frac{\Delta t}{\Delta x} = -\alpha \phi_j$$

TABLE 4. Phase speed ratio for the integrated flux form.

Order	Courant number						
	0.01	0.1	0.3	0.5	0.7	0.9	1.0
$4\Delta x$							
1	0.643	0.704	0.859	1.000	1.060	1.033	1.000
2	0.637	0.641	0.676	0.749	0.856	0.964	1.000
3	0.798	0.818	0.868	0.915	0.943	0.947	0.942
4	0.957	0.972	0.992	0.990	0.973	0.951	0.942
5	0.856	0.865	0.887	0.909	0.924	0.932	0.933
6	0.916	0.922	0.933	0.937	0.936	0.934	0.933
7	0.881	0.884	0.895	0.908	0.919	0.927	0.931
8	0.906	0.908	0.915	0.920	0.924	0.928	0.931
9	0.891	0.893	0.899	0.908	0.916	0.925	0.930
10	0.902	0.904	0.908	0.913	0.919	0.926	0.930
$8\Delta x$							
1	0.903	0.926	0.970	1.000	1.013	1.008	1.000
2	0.900	0.901	0.910	0.928	0.953	0.984	1.000
3	0.966	0.968	0.973	0.976	0.978	0.978	0.978
4	0.986	0.985	0.984	0.982	0.980	0.978	0.978
5	0.974	0.974	0.974	0.975	0.976	0.977	0.977
6	0.976	0.976	0.976	0.976	0.976	0.977	0.977
7	0.974	0.974	0.975	0.975	0.976	0.976	0.977
8	0.975	0.975	0.975	0.975	0.976	0.976	0.977
9	0.974	0.975	0.975	0.975	0.976	0.976	0.977
10	0.975	0.975	0.975	0.976	0.976	0.976	0.977

nomial of one order less than the desired scheme, only contains the interactions between ORD points. Thus, it is not guaranteed that the subtraction of two fluxes will produce the advective form. This is the case for ORD = 3 through 10.

Although this inconsistency between the flux and advective forms does not affect the conservation properties of the flux form, it does affect the accuracy. A stability analysis was performed on the flux form assuming a constant u and Δx (Tables 3 and 4). Both amplitude and phase errors are increased significantly from the advective form (Tables 1 and 2).

Fortunately, by *requiring* that a flux form reduce to the advective form for a constant grid spacing and velocity, a new form can be derived that has identical errors to the advective form in the linear stability analysis. A constant grid flux form can be obtained algebraically in the following manner. We can write

$$\left.\begin{array}{l} F_{j+1/2} = \sum_m b_m \phi_{j+1+m}^n \\[2ex] F_{j-1/2} = \sum_m b_m \phi_{j+m}^n \end{array}\right\}$$

ORD = 2:

$$F_{j+1/2}\frac{\Delta t}{\Delta x} = \alpha/2(-\phi_j - \phi_{j+1}) + \alpha^2/2(-\phi_j + \phi_{j+1})$$

ORD = 3:

$$F_{j+1/2}\frac{\Delta t}{\Delta x} = \alpha/6(\phi_{j-1} - 5\phi_j - 2\phi_{j+1})$$
$$+ \alpha^2/2(-\phi_j + \phi_{j+1})$$
$$+ \alpha^3/6(-\phi_{j-1} + 2\phi_j - \phi_{j+1})$$

ORD = 4:

$$F_{j+1/2}\frac{\Delta t}{\Delta x} = \alpha/12(\phi_{j-1} - 7\phi_j - 7\phi_{j+1} + \phi_{j+2})$$
$$+ \alpha^2/24(\phi_{j-1} - 15\phi_j + 15\phi_{j+1} - \phi_{j+2})$$
$$+ \alpha^3/12(-\phi_{j-1} + \phi_j + \phi_{j+1} - \phi_{j-2})$$
$$+ \alpha^4/24(-\phi_{j-1} + 3\phi_j - 3\phi_{j+1} + \phi_{j+2})$$

ORD = 5:

$$F_{j+1/2}\frac{\Delta t}{\Delta x} = \alpha/60(-2\phi_{j-2} + 13\phi_{j-1} - 47\phi_j$$
$$- 27\phi_{j+1} + 3\phi_{j+2})$$
$$+ \alpha^2/24(\phi_{j-1} - 15\phi_j + 15\phi_{j+1} - \phi_{j+2})$$
$$+ \alpha^3/24(\phi_{j-2} - 6\phi_{j-1} + 8\phi_j - 2\phi_{j+1} - \phi_{j+2})$$
$$+ \alpha^4/24(-\phi_{j-1} + 3\phi_j - 3\phi_{j+1} + \phi_{j+2})$$
$$+ \alpha^5/120(-\phi_{j-2} + 4\phi_{j-1} - 6\phi_j$$
$$+ 4\phi_{j+1} - \phi_{j+2})$$

ORD = 6:

$$F_{j+1/2}\frac{\Delta t}{\Delta x} = \alpha/60(-\phi_{j-2} + 8\phi_{j-1} - 37\phi_j - 37\phi_{j+1}$$
$$+ 8\phi_{j+2} - \phi_{j+3})$$
$$+ \alpha^2/360(-2\phi_{j-2} + 25\phi_{j-1} - 245\phi_j$$
$$+ 245\phi_{j+1} - 25\phi_{j+2} + 2\phi_{j+3})$$
$$+ \alpha^3/48(\phi_{j-2} - 7\phi_{j-1} + 6\phi_j + 6\phi_{j+1}$$
$$- 7\phi_{j+2} + \phi_{j+3})$$
$$+ \alpha^4/144(\phi_{j-2} - 11\phi_{j-1} + 28\phi_j - 28\phi_{j+1}$$
$$+ 11\phi_{j+2} - \phi_{j+3})$$
$$+ \alpha^5/240(-\phi_{j-2} + 3\phi_{j-1} - 2\phi_j - 2\phi_{j+1}$$
$$+ 3\phi_{j+2} - \phi_{j+3})$$
$$+ \alpha^6/720(-\phi_{j-2} + 5\phi_{j-1} - 10\phi_j + 10\phi_{j+1}$$
$$- 5\phi_{j+2} + \phi_{j+3}).$$

The expressions for order 7 through 10 are given in the Appendix.

The linear stability analysis for the constant grid flux schemes is equivalent to the analysis in Tables 1 and 2. Unfortunately, this technique cannot be extended to a variable grid spacing, as the coefficients for ϕ_{j+i} are nonlinear functions of the grid spacings.

4. Multi-dimensional advection

As pointed out by Leith (1965), the second-order Crowley scheme is unstable in two dimensions if the advective operators are applied simultaneously, that is, if we approximate $\phi_{j,k}^{n+1}$ with

$$\phi_{j,k}^{n+1} = P_j[x_{j,k} - u\Delta t, \phi_{j,k}^n] + P_k[y_{j,k} - v\Delta t, \phi_{j,k}^n]$$

where u and v are perpendicular velocity components and the subscript on P indicates the direction in which the spline is applied. All orders of upstream Lagrangian schemes show the same behavior. This instability is caused by the neglect of the cross-derivative terms in the Taylor expansion, as mentioned by Leith (1965) and Smolarkiewicz (1982). The simultaneous or combined scheme can be viewed as fitting two one-dimensional polynomials to a set of data points, instead of a polynomial surface, consequently excluding a great deal of data from the domain of dependence.

To control this instability, two methods have been used. Leith (1965) and Crowley (1968), among others, used the method of fractional timesteps or "time-splitting," which consists of two consecutive passes through the field. Thus

$$\phi_{j,k}^* = P_j[x_{j,k} - u\Delta t, \phi_{j,k}^n]$$
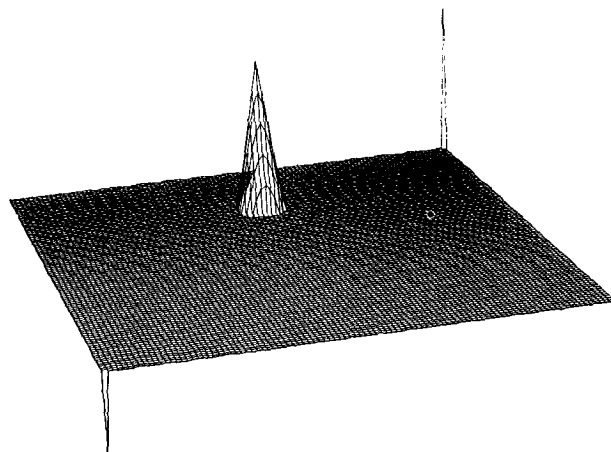$$\phi_{j,k}^{n+1} = P_k[x_{j,k} - v\Delta t, \phi_{j,k}^*].$$

FIG. 1. The initial condition for the rotating cone experiments. The scale in the upper right corner is the initial height of the cone.
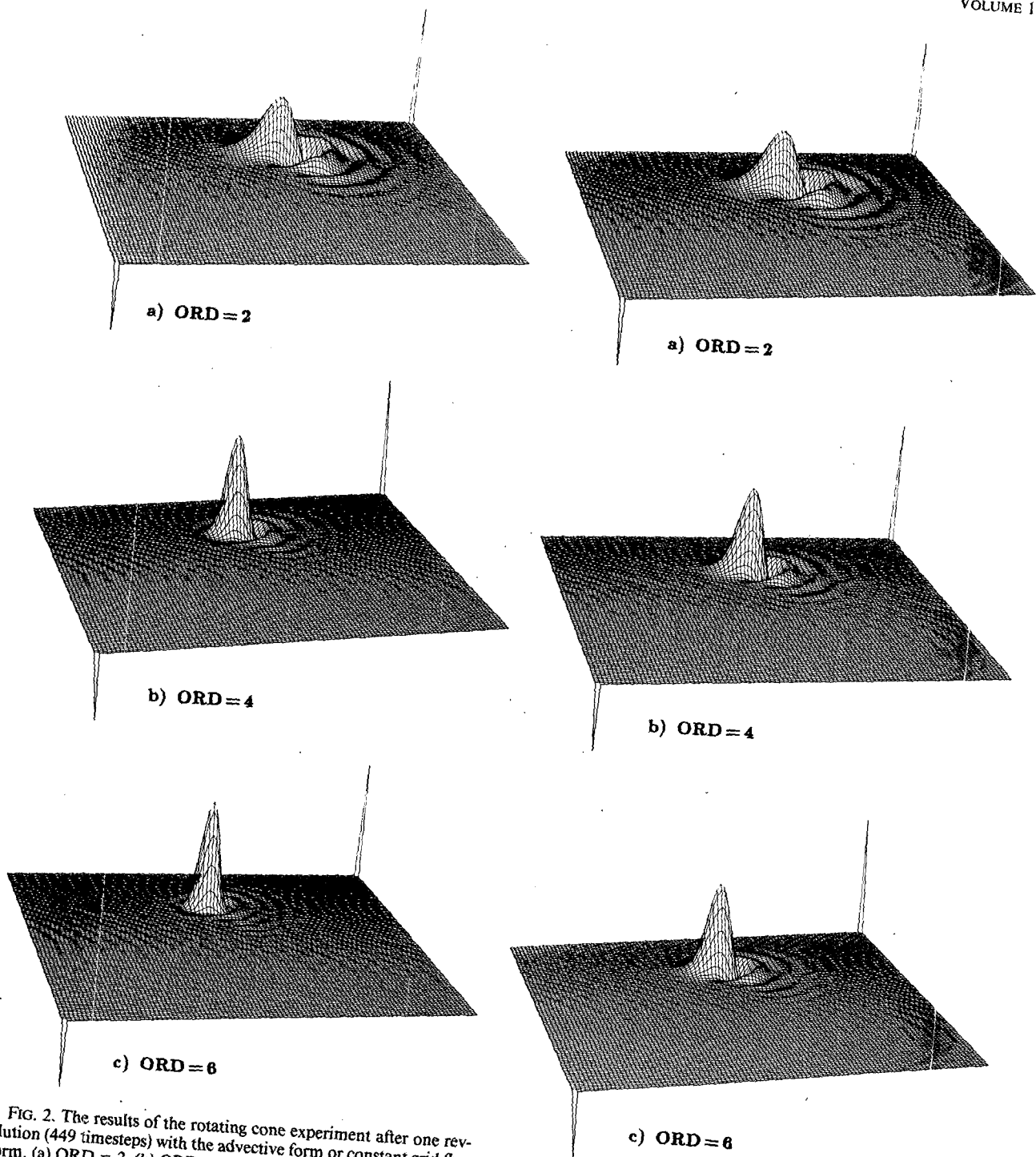
a) ORD = 2

b) ORD = 4

c) ORD = 6

FIG. 2. The results of the rotating cone experiment after one revolution (449 timesteps) with the advective form or constant grid flux form. (a) ORD = 2, (b) ORD = 4 and (c) ORD = 6.

a) ORD = 2

b) ORD = 4

c) ORD = 6

FIG. 3. As in Fig. 2 but with the integrated flux form.

Alternatively, Smolarkiewicz (1982) explicitly added the cross-derivative terms to the Crowley scheme. This method was also tested by Schlesinger (1985).

We have chosen to use the time-split scheme for several reasons:

• The methodology in section 2 could possibly be extended to multidimensional polynomial surface fitting. However, the resulting scheme would use at least $(ORD + 1)^m$ data points, where m is the number of dimensions, while the time-split technique only uses

TABLE 5. Results from the rotating cone experiment after one revolution (449 time steps); the initial amplitude was 10 units.

Order	ϕ_{max}	ϕ_{min}	$\Sigma \phi_{neg}/\Sigma \phi_0$	$\Sigma \phi^2/\Sigma \phi_0{}^2$	CPU
		Advective form and constant grid flux form			
1	0.56	0.00	0.00	0.056	1.1
2	4.57	−1.83	−0.70	0.774	1.0
3	5.43	−0.21	−0.10	0.658	1.8
4	8.04	−0.84	−0.16	0.963	1.5
5	8.13	−0.22	−0.16	0.939	3.7
6	8.78	−0.26	−0.07	0.990	3.2
7	8.66	−0.15	−0.04	0.986	7.8
8	8.69	−0.21	−0.05	0.994	5.9
9	8.67	−0.13	−0.03	0.993	13.6
10	8.60	−0.18	−0.05	0.995	9.4
		Integrated flux form			
1	0.56	0.00	0.00	0.056	1.1
2	4.57	−1.83	−0.70	0.774	1.0
3	5.40	−0.62	−0.17	0.682	1.8
4	6.80	−1.50	−0.35	0.916	1.5
5	7.11	−1.20	−0.24	0.902	3.7
6	7.24	−1.36	−0.28	0.930	3.2
7	7.30	−1.33	−0.26	0.929	7.8
8	7.30	−1.35	−0.27	0.932	5.9
9	7.31	−1.35	−0.26	0.932	13.6
10	7.31	−1.36	−0.27	0.932	9.4

m(ORD + 1) points. For a second-order scheme, this may be reasonable, but for higher-order schemes the cost becomes prohibitive.

- Smolarkiewicz (1982) favored cross derivatives over time-splitting because time-splitting requires more data transfer than computing cross derivatives. However, time-splitting requires far less computation since, as with the multidimensional surface fit, the cross term scheme requires (ORD + 1)^m points. Also, a model can be engineered so that there need not be any additional data transfer for the time-split schemes.

- The stability criterion for the time-split scheme does not change from one to several dimensions.

a. Rotational flow field tests

The upstream advective schemes using time-splitting were tested with the classic rotating cone experiment. The initial condition is shown in Fig. 1. The domain consisted of an unstaggered grid of 101 by 101 points with a pure rotational, nondivergent velocity field having an angular velocity of 0.2. The cone had an initial amplitude of 10 units and a base diameter of 10Δx. The Courant number at the center of the cone was 0.35. The lateral boundaries were held constant, while second-order advection and fluxes were computed at points near the boundary where higher-order approximations could not be computed.

Figure 2 shows the cone after one revolution (449 time steps) with the advective form and ORD = 2, 4 and 6. Figure 3 contains the same order schemes with

the integrated flux forms. Table 5 summarizes the results for all schemes. Constant grid flux forms were also tested. We expected the behaviors of constant grid flux and advective forms to be similar, given the requirement that the constant grid form reduce to the advective form for constant spacing and given that the velocities were relatively uniform across adjacent grid points in the rotating tests. Indeed, the results of the tests were identical to eight significant figures for both forms.

The results in Table 5 are consistent with the linear stability analysis. The first-order schemes almost completely damp the cone after one revolution. The second-order schemes maintain more of the amplitude but, because of the large dispersion errors, a trailing wake is produced which contains much of the original amplitude of the cone. As the order of the scheme increases, both errors are reduced; less damping maintains more of the initial maximum of the cone while less dispersion decreases the negative amount of material produced by the scheme. A higher-order scheme, although not maintaining a positive definite field, will reduce the problem of negative quantities dramatically.

Comparing the constant grid flux form and the integrated flux form, the results are again consistent with the linear stability analysis. The lower maximums produced by the integrated flux forms are evidence of the greater damping and the larger negative quantities are evidence of the higher dispersion errors.

Relative efficiencies for various order schemes are also listed in Table 5. All schemes were completely vectorized (the odd-ordered schemes required the computation of two fluxes per point per direction). Again, it appears that the sixth-order scheme gives a good balance between accuracy and efficiency.

b. Deformational flow field tests

The second-, fourth- and sixth-order schemes were tested in the deformational flow field given by Smolarkiewicz (1982). A grid of 101 by 101 points was used with the velocity field defined from the streamfunction given in Fig. 4. A cone of amplitude 10 and base diameter of 30 Δx was initially centered in the domain as shown in Fig. 5. Two different time steps, yielding maximum Courant numbers of 0.14 and 0.70, were used. No damping or filtering of any kind was employed.

The solutions after 3000 time steps are shown in Figs. 6 through 9. Figure 6a is the sixth-order advective form with the lower Courant number and Fig. 6b is the same scheme with the higher Courant number. All orders tested, including eighth and tenth orders, show this same highly unstable behavior with the advective form in this deformational flow field.

Figure 7 is the sixth-order constant grid flux form after 3000 time steps with the higher Courant number. Along with the integrated flux form this same pattern

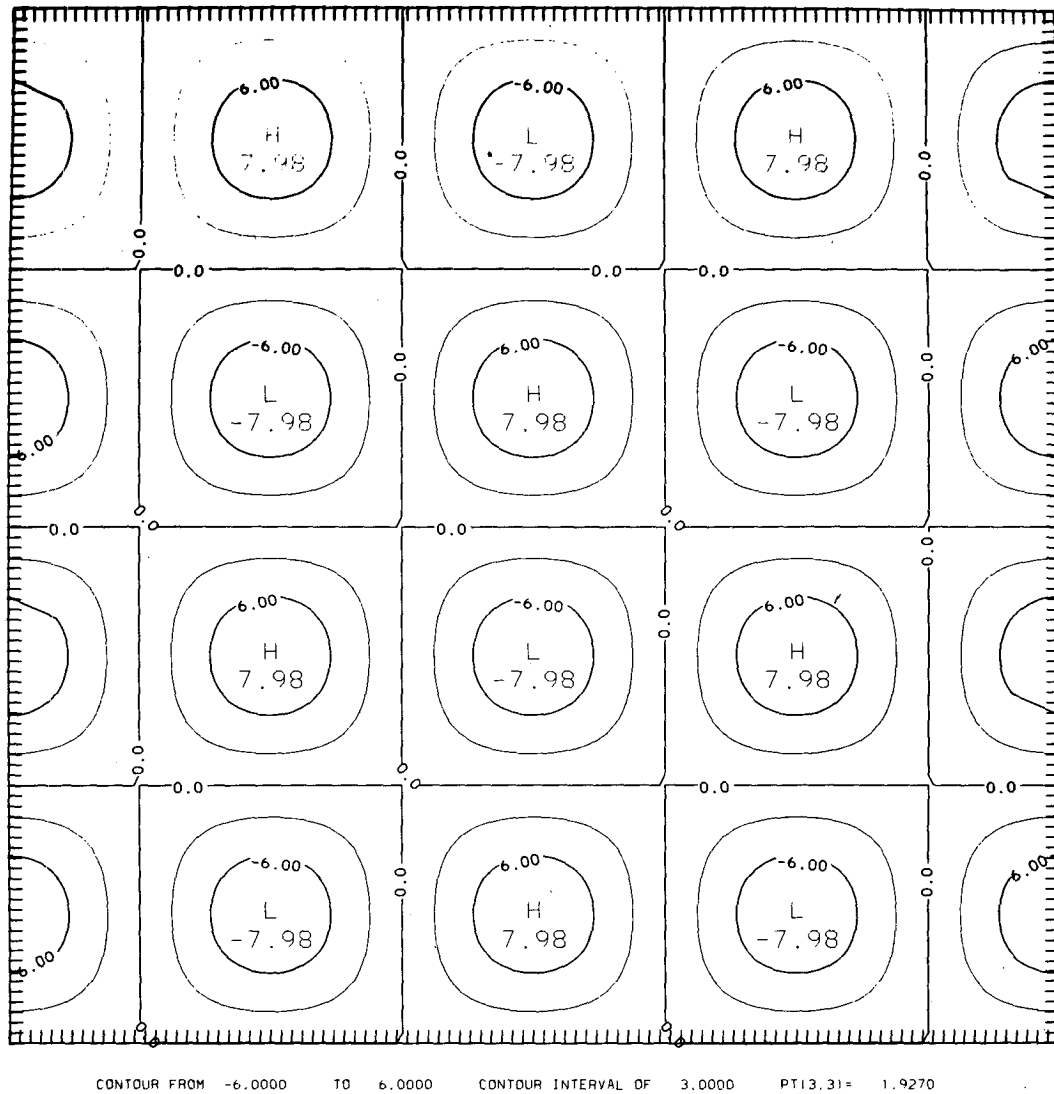CONTOUR FROM -6.0000 TO 6.0000 CONTOUR INTERVAL OF 3.0000 PT(3.31)= 1.9270

FIG. 4. Streamfunction for the deformational flow field tests.

was produced for all orders of schemes. Although the field is unstable, the rate of instability is much less than the advective form.

The domain, as a whole, was stable for the flux forms run with the lower Courant number. Figure 8 is the integrated flux form with ORD = 2, 4 and 6 while Fig. 9 is the constant grid flux form with ORD = 4 and 6. Even though the domain was stable, there was some evidence of local instability. These results are consistent with Petschek and Libersky (1975) who showed that the second-order time-split flux form was unstable in a particular deformational flow field and that the instability increased with increasing Courant numbers. The results for all orders of advective and flux forms tested are summarized in Table 6.

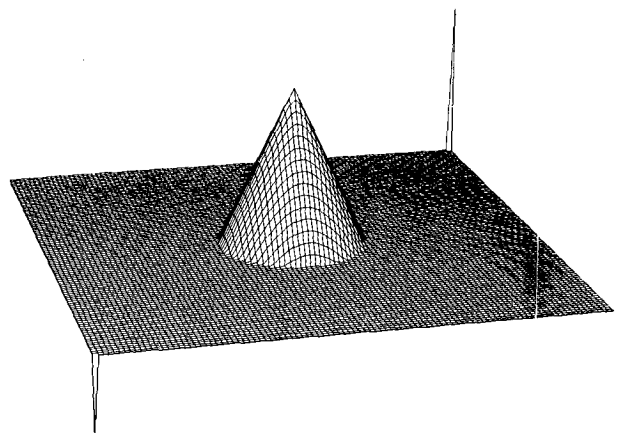As pointed out by Smolarkiewicz (1982), this flow

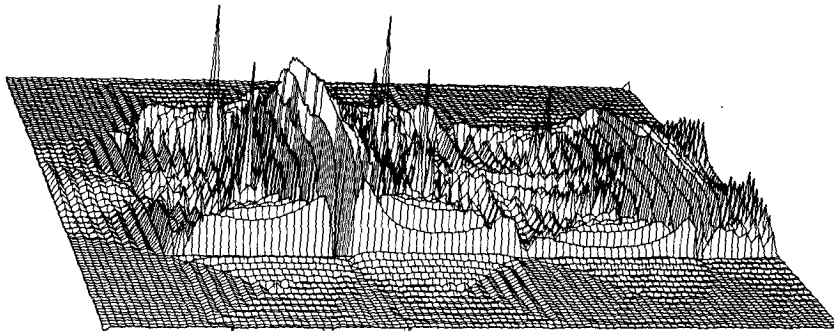FIG. 5. The initial condition for the deformational tests.

a) $\alpha_{max} = .14$
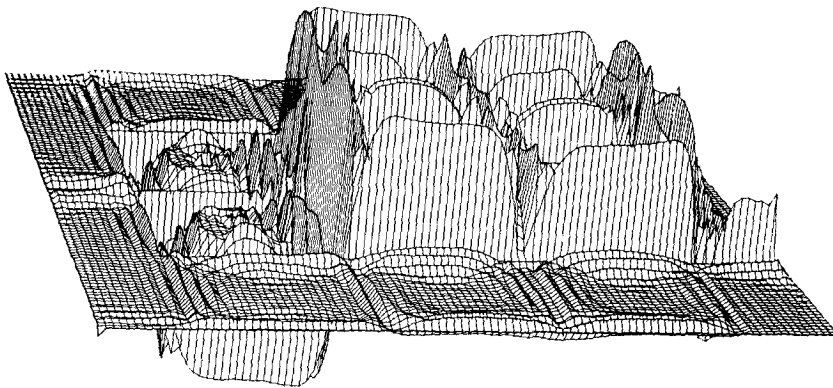
b) $\alpha_{max} = .70$

FIG. 6. Results of the deformational tests after 3000 time steps with the sixth-order advective form: (a) Courant number = 0.14, (b) Courant number = 0.70.
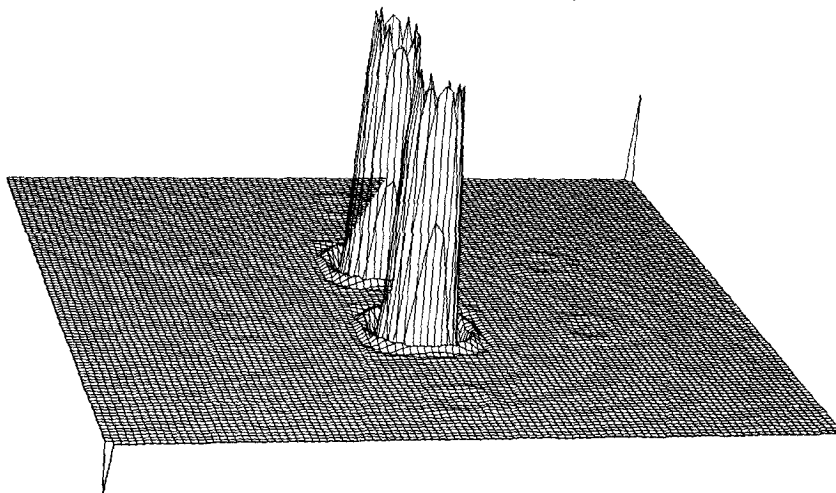
$\alpha_{max} = .70$

FIG. 7. Results of the deformational tests after 3000 time steps with the sixth-order constant grid flux form. Courant number = 0.70.

a) ORD = 2

b) ORD = 4

c) ORD = 6

FIG. 8. Results of the deformational tests after 3000 time steps with the integrated flux form. Courant number = 0.14. (a) ORD = 2, (b) ORD = 4 and (c) ORD = 6.

FIG. 9. As in Fig. 8 but with the constant grid flux form for ORD = 4 and 6 only.
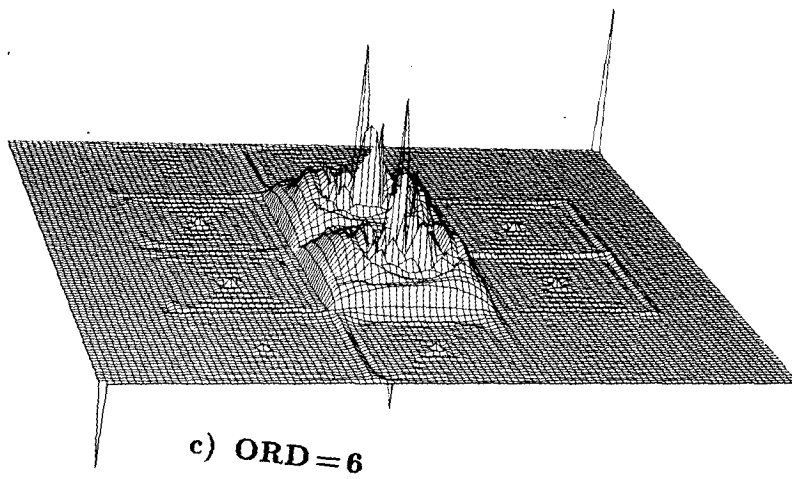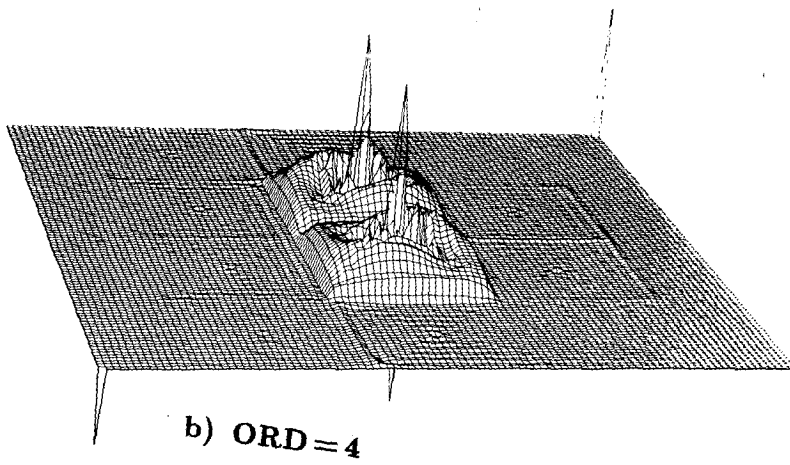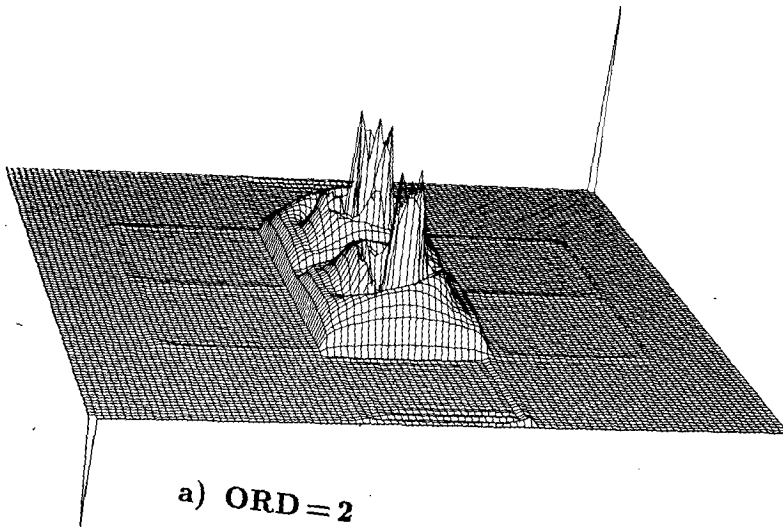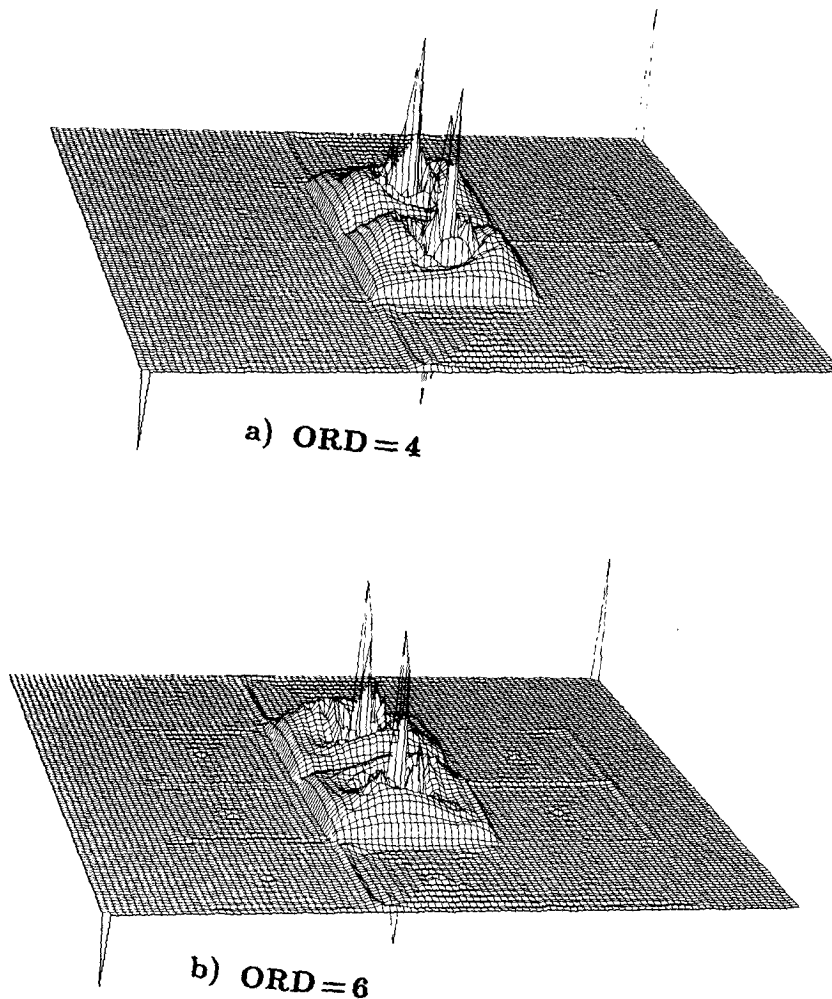
field has a large degree of deformation. As a result, this is a very stringent test of the schemes. In most atmospheric modeling applications, these values of deformation are never achieved, or if they are, they do not exist for very long. However, if large deformations are expected or prespecified in an application, the use of a flux form should be considered over the advective form. In addition, the instabilities can be reduced by choosing a smaller Courant number.

4. Summary

The methodology used by Crowley (1968) to derive an advective scheme by upstream interpolation along a polynomial has been extended to higher orders, and a new flux form that can be used for constant grid spacing has been developed. The advective form and constant grid flux form have identical linear stability characteristics in one dimension, while the integrated flux form has greater amplitude and phase errors for schemes of order 3 and higher.

When the schemes were extended to two dimensions using time-splitting and tested in rotational and deformational flow fields, the results were consistent with the one-dimensional stability analyses. The advective form and constant grid flux form had smaller amplitude and dispersion errors than the integrated flux form in the rotational tests. In the deformational tests, the advective form was absolutely unstable while the stability of the flux forms was dependent on the Courant number.

For the ten orders of schemes tested, the sixth-order advective scheme appears to be the best balance between accuracy and efficiency. For constant grid applications, the corresponding sixth-order constant grid flux form is equally desirable, and has the added ad-

TABLE 6. Results from the deformational flow experiments after 3000 time steps.

	Order	ϕ_{max}	ϕ_{min}	$\Sigma \phi_{neg}/\Sigma \phi_0$	$\Sigma \phi^2/\Sigma \phi_0^2$
		Advective form			
$\alpha_{max} = 0.14$	2	55.65	−58.54	−11.59	117.573
	4	192.30	−208.59	−33.07	810.463
	6	478.98	−496.29	−83.71	4831.170
$\alpha_{max} = 0.7$	2	206.17	−203.71	−36.69	1810.561
	4	203.36	−200.01	−45.00	2505.305
	6	226.59	−221.18	−50.14	2876.209
		Constant grid flux form			
$\alpha_{max} = 0.14$	2	7.48	−5.44	−0.05	0.551
	4	12.83	−9.51	−0.05	0.514
	6	11.66	−8.20	−0.06	0.509
$\alpha_{max} = 0.7$	2	18.04	−0.92	−0.06	2.436
	4	24.42	−6.64	−0.09	3.566
	6	26.95	−7.41	−0.11	4.157
		Integrated flux form			
$\alpha_{max} = 0.14$	2	7.48	−5.44	−0.05	0.551
	4	12.45	−9.17	−0.05	0.534
	6	13.46	−9.98	−0.06	0.529
$\alpha_{max} = 0.7$	2	18.04	−0.92	−0.06	2.436
	4	21.67	−4.94	−0.08	3.197
	6	24.61	−4.30	−0.08	3.421

vantages of being less unstable than the advective form in deformational flow fields and conservative in nondivergent fields. In any case, a sixth-order approximation dramatically decreases errors over lower-order upstream schemes. Advection costs are relatively small in a three-dimensional atmospheric model with detailed physics, and consequently the expense of sixth-order schemes is not prohibitive. It appears that the sixth-order schemes are well-suited for many atmospheric modeling applications where advection plays a significant role.

APPENDIX

Advective schemes of order 7 through 10

The expressions for the advective schemes and fluxes of order 7 through 10 are described in tabular form below. The table is arranged with the coefficient of each order of term in the first column and the grid point horizontal. For example, the second-order term for the seventh-order advective form would be

$$\frac{\alpha^2}{360}(2\phi_{j-3} - 27\phi_{j-2} + 270\phi_{j-1} - 490\phi_j + 270\phi_{j+1} + 27\phi_{j+2} + 2\phi_{j+3}).$$

The entire expression then would be the sum of all orders of terms.

1. Advective form

The advective form of the schemes is given by

$$\phi_j^{n+1} = \phi_j^n + G(x_j, \phi^n)$$

and $G(x_j, \phi^n)$ is given in the following tables for orders 7 through 10. A positive velocity is assumed for the odd-ordered schemes.

ORD = 7:

	ϕ_{j-4}	ϕ_{j-3}	ϕ_{j-2}	ϕ_{j-1}	ϕ_j	ϕ_{j+1}	ϕ_{j+2}	ϕ_{j+3}
$\alpha/420$	−3	28	−126	420	−105	−252	42	−4
$\alpha^2/360$	0	2	−27	270	−490	270	−27	2
$\alpha^3/720$	7	−64	267	−440	245	48	−71	8
$\alpha^4/144$	0	−1	12	−39	56	−39	12	−1
$\alpha^5/720$	−2	17	−54	85	−70	27	−2	−1
$\alpha^6/720$	0	1	−6	15	−20	15	−6	1
$\alpha^7/5040$	1	−7	21	−35	35	−21	7	−1

ORD = 8:

	ϕ_{j-4}	ϕ_{j-3}	ϕ_{j-2}	ϕ_{j-1}	ϕ_j	ϕ_{j+1}	ϕ_{j+2}	ϕ_{j+3}	ϕ_{j+4}
$\alpha/840$	-3	32	-168	672	0	-672	168	-32	3
$\alpha^2/10080$	-9	128	-1008	8064	-14350	8064	-1008	128	-9
$\alpha^3/1440$	7	-72	338	-488	0	488	-338	72	-7
$\alpha^4/5760$	7	-96	676	-1952	2730	-1952	676	-96	7
$\alpha^5/720$	-1	9	-26	29	0	-29	26	-9	1
$\alpha^6/2880$	-1	12	-52	116	-150	116	-52	12	-1
$\alpha^7/10080$	1	-6	14	-14	0	14	-14	6	-1
$\alpha^8/40320$	1	-8	27	-56	70	-56	28	-8	1

ORD = 9:

	ϕ_{j-5}	ϕ_{j-4}	ϕ_{j-3}	ϕ_{j-2}	ϕ_{j-1}	ϕ_j	ϕ_{j+1}	ϕ_{j+2}	ϕ_{j+3}	ϕ_{j+4}
$\alpha/2520$	4	-45	240	-840	2520	-504	-1680	360	-60	5
$\alpha^2/10080$	0	-9	128	-1008	8064	-14350	8064	-1008	128	-9
$\alpha^3/90720$	-205	2286	-11916	38514	-56574	25830	13524	-13914	2691	-236
$\alpha^4/5760$	0	7	-96	676	-1952	2730	-1952	676	-96	7
$\alpha^5/17280$	13	-141	684	-1716	2334	-1638	396	156	-99	11
$\alpha^6/2880$	0	-1	12	-52	116	-150	116	-52	12	-1
$\alpha^7/60480$	-5	51	-216	504	-714	630	-336	96	-9	-1
$\alpha^8/40320$	0	1	-8	28	-56	70	-56	28	-8	1
$\alpha^9/362880$	1	-9	36	-84	126	-126	84	-36	9	-1

ORD = 10:

	ϕ_{j-5}	ϕ_{j-4}	ϕ_{j-3}	ϕ_{j-2}	ϕ_{j-1}	ϕ_j	ϕ_{j+1}	ϕ_{j+2}	ϕ_{j+3}	ϕ_{j+4}	ϕ_{j+5}
$\alpha/2520$	2	-25	150	-600	2100	0	-2100	600	-150	25	-2
$\alpha^2/50400$	8	-125	1000	-6000	42000	-73766	42000	-6000	1000	-125	8
$\alpha^3/181440$	-205	2522	-14607	52428	-70098	0	70098	-52428	14607	-2522	205
$\alpha^4/362880$	-82	1261	-9738	52428	-140196	192654	-140196	52428	-9738	1261	-82
$\alpha^5/34560$	13	-152	783	-1872	1938	0	-1938	1872	-783	152	-13
$\alpha^6/172800$	13	-190	1305	-4680	9690	-12276	9690	-4680	1305	-190	13
$\alpha^7/120960$	-5	52	-207	408	-378	0	378	-408	207	-52	5
$\alpha^8/120960$	-1	13	-69	204	-378	462	-378	204	-69	13	-1
$\alpha^9/725760$	1	-8	27	-48	42	0	-42	48	-27	8	-1
$\alpha^{10}/3628800$	1	-10	45	-120	210	-252	210	-120	45	-10	1

2. Integrated flux form

The flux form of the schemes is given by $\phi_j^{n+1} = \phi_j^n + (\Delta t/\Delta x)(F_{j+1/2} - F_{j-1/2})$ and $F_{j+1/2}$ $(\Delta t/\Delta x)$ is given in the following tables for orders 7 through 10. A positive velocity is assumed for the odd-ordered schemes.

ORD = 7:

	ϕ_{j-3}	ϕ_{j-2}	ϕ_{j-1}	ϕ_j	ϕ_{j+1}	ϕ_{j+2}	ϕ_{j+3}
$\alpha/1024$	5	-42	175	-700	-525	70	-7
$\alpha^2/3840$	0	-9	125	-2250	2250	-125	9
$\alpha^3/34560$	-259	2154	-8565	9260	195	-3126	341
$\alpha^4/192$	0	1	-13	34	-34	13	-1
$\alpha^5/2880$	7	-54	141	164	81	-6	-5
$\alpha^6/720$	0	-1	5	-10	10	-5	1
$\alpha^7/5040$	-1	6	-15	20	-15	6	-1

ORD = 8:

	ϕ_{j-3}	ϕ_{j-2}	ϕ_{j-1}	ϕ_j	ϕ_{j+1}	ϕ_{j+2}	ϕ_{j+3}	ϕ_{j+4}
$\alpha/2048$	5	-49	245	-1225	-1225	245	-49	5
$\alpha^2/215040$	75	-1029	8575	-128625	128625	-8575	1029	-75
$\alpha^3/69120$	-259	2495	-11691	9455	9455	-11691	2495	-259
$\alpha^4/46080$	-37	499	-3897	9455	-9455	3897	-499	37
$\alpha^5/5760$	7	-59	135	-83	-83	135	-59	7
$\alpha^6/17280$	5	-59	225	-415	415	-225	59	-5
$\alpha^7/10080$	-1	5	-9	5	5	-9	5	-1
$\alpha^8/40320$	-1	7	-21	35	-35	21	-7	1

ORD = 9:

	ϕ_{j-4}	ϕ_{j-3}	ϕ_{j-2}	ϕ_{j-1}	ϕ_j	ϕ_{j+1}	ϕ_{j+2}	ϕ_{j+3}	ϕ_{j+4}
$\alpha/32768$	-35	360	-1764	5880	-22050	-17640	2940	-504	45
$\alpha^2/215040$	0	75	-1029	8575	-128625	128625	-8575	1029	-75
$\alpha^3/1935360$	-3229	-33084	160272	-508172	490770	83916	-236936	44028	-4023
$\alpha^4/46080$	0	-37	499	-3897	9455	-9455	3897	-499	37
$\alpha^5/230400$	-141	1408	-6308	13296	-13190	4576	1452	-1232	139
$\alpha^6/17280$	0	5	-59	225	-415	415	-225	59	-5
$\alpha^7/40320$	3	-28	104	-204	230	-148	48	-4	-1
$\alpha^8/40320$	0	-1	7	-21	35	-35	21	-7	1
$\alpha^9/362880$	-1	8	-28	56	-70	56	-28	8	-1

ORD = 10:

	ϕ_{j-4}	ϕ_{j-3}	ϕ_{j-2}	ϕ_{j-1}	ϕ_j	ϕ_{j+1}	ϕ_{j+2}	ϕ_{j+3}	ϕ_{j+4}	ϕ_{j+5}
$\alpha/65536$	-35	405	-2268	8820	-39690	-39690	8820	-2268	405	-35
$\alpha^2/20643840$	-1225	18225	-142884	926100	-12502350	12502350	-926100	142884	-18225	1225
$\alpha^3/3870720$	3229	-37107	204300	-745108	574686	574686	-745108	204300	-37107	3229
$\alpha^4/23224320$	3229	-47709	367740	-2235324	5172174	-5172174	2234324	-367740	47709	-3229
$\alpha^5/460880$	-141	1547	-7540	14748	-8614	-8614	14748	-7540	1547	-141
$\alpha^6/829440$	-47	663	-4524	14748	-25842	25842	-14748	4524	-663	47
$\alpha^7/80640$	3	-29	100	-156	82	82	-156	100	-29	3
$\alpha^8/967680$	7	-87	420	-1092	1722	-1722	1092	-420	87	-7
$\alpha^9/725760$	-1	7	-20	28	-14	-14	28	-20	7	-1
$\alpha^{10}/3628800$	-1	9	-36	84	-126	126	-84	36	-9	1

3. Constant grid flux form

The expression for $F_{j+1/2}(\Delta t/\Delta x)$ for the constant grid flux form is given in the tables below for orders 7 through 10. A positive velocity is assumed for the odd-ordered schemes.

ORD = 7:

	ϕ_{j-3}	ϕ_{j-2}	ϕ_{j-1}	ϕ_j	ϕ_{j+1}	ϕ_{j+2}	ϕ_{j+3}
$\alpha/420$	3	-25	101	-319	-214	38	-4
$\alpha^2/360$	0	-2	25	-245	245	-25	2
$\alpha^3/720$	-7	57	-210	230	-15	-63	8
$\alpha^4/144$	0	1	-11	28	-28	11	-1
$\alpha^5/720$	2	-15	39	-46	24	-3	-1
$\alpha^6/720$	0	-1	5	-10	10	-5	1
$\alpha^7/5040$	-1	6	-15	20	-15	6	-1

ORD = 8:

	ϕ_{j-3}	ϕ_{j-2}	ϕ_{j-1}	ϕ_j	ϕ_{j+1}	ϕ_{j+2}	ϕ_{j+3}	ϕ_{j+4}
$\alpha/840$	3	-29	139	-533	-533	139	-29	3
$\alpha^2/10080$	9	-119	889	-7175	7175	-899	119	-9
$\alpha^3/1440$	-7	65	-273	215	215	-273	65	-7
$\alpha^4/5760$	-7	89	-587	1365	-1365	587	-89	7
$\alpha^5/720$	1	-8	18	-11	-11	18	-8	1
$\alpha^6/2880$	1	-11	41	-75	75	-41	11	-1
$\alpha^7/10080$	-1	5	-9	5	5	-9	5	-1
$\alpha^8/40320$	-1	7	-21	35	-35	21	-7	1

ORD = 9:

	ϕ_{j-4}	ϕ_{j-3}	ϕ_{j-2}	ϕ_{j-1}	ϕ_j	ϕ_{j+1}	ϕ_{j+2}	ϕ_{j+3}	ϕ_{j+4}
$\alpha/2520$	-4	41	-199	641	-1879	-1375	305	-55	5
$\alpha^2/10080$	0	9	-119	889	-7175	7175	-889	119	-9
$\alpha^3/90720$	205	-2081	9835	-28679	27895	2065	-11459	2455	-236
$\alpha^4/5760$	0	-7	89	-587	1365	-1365	587	-89	7
$\alpha^5/17280$	-13	128	-556	1160	-1174	464	68	-88	11
$\alpha^6/2880$	0	1	-11	41	-75	75	-41	11	-1
$\alpha^7/60480$	5	-46	170	-334	380	-250	86	-10	-1
$\alpha^8/40320$	0	-1	7	-21	35	-35	21	-7	1
$\alpha^9/362880$	-1	8	-28	56	-70	56	-28	8	-1

ORD = 10:

	ϕ_{j-4}	ϕ_{j-3}	ϕ_{j-2}	ϕ_{j-1}	ϕ_j	ϕ_{j+1}	ϕ_{j+2}	ϕ_{j+3}	ϕ_{j+4}	ϕ_{j+5}
$\alpha/2520$	-2	23	-127	473	-1627	-1627	473	-127	23	-2
$\alpha^2/50400$	-8	117	-883	5117	-36883	36883	-5117	883	-117	8
$\alpha^3/181440$	205	-2317	12290	-40138	29960	29960	-40138	12290	-2317	205
$\alpha^4/362880$	82	-1179	8559	-43869	96327	-96327	43869	-8559	1179	-82
$\alpha^5/34560$	-13	139	-644	1228	-710	-710	1228	-644	139	-13
$\alpha^6/172800$	-13	177	-1128	3552	-6138	6138	-3552	1128	-177	13
$\alpha^7/120960$	5	-47	160	-248	130	130	-248	160	-47	5
$\alpha^8/120960$	1	-12	57	-147	231	-231	147	-57	12	-1
$\alpha^9/725760$	-1	7	-20	28	14	-14	28	-20	7	-1
$\alpha^{10}/3628800$	-1	9	-36	84	-126	126	-84	36	-9	1

REFERENCES

Chen, C. H., and H. D. Orville, 1980: Effects of mesoscale convergence on cloud convection. *J. Appl. Meteor.,* **19**, 256–274.

Crowley, W. P., 1968: Numerical advection experiments. *Mon. Wea. Rev.,* **96**, 1–11.

Flatau, P. J., John P. Boyd and W. R. Cotton, 1986: Symbolic algebra in applied mathematics and geophysical fluid dynamics—REDUCE examples. Dept. of Atmospheric Science, Colorado State University, 153 pp.

Hearn, A. C., 1984: *REDUCE User's Manual, Ver. 3.0.* Rand Publ. CP78(4/83), The RAND Corporation, 107 pp.

Leith, C. E., 1965: Numerical simulation of the earth's atmosphere. Applications in hydrodynamics, Vol. 4, *Methods in Computational Physics,* Academic Press, 1–28.

Molenkamp, C. R., 1968: Accuracy of finite-difference methods applied to the advection equation. *J. Appl. Meteor.,* **7**, 160–167.

Orville, H. D., and F. J. Kopp, 1977: Numerical simulation of the life history of a hailstorm. *J. Atmos. Sci.,* **34**, 1596–1618.

Petschek, A. G., and L. D. Libersky, 1975: Stability, accuracy, and improvement of Crowley advection schemes. *Mon. Wea. Rev.,* **103**, 1104–1109.

Schlesinger, R. E., 1985: Effects of upstream-biased third-order space correction terms on multidimensional Crowley advection schemes. *Mon. Wea. Rev.,* **113**, 1109–1130.

Smolarkiewicz, P. K., 1982: The multidimensional Crowley advection scheme. *Mon. Wea. Rev.,* **110**, 1968–1983.

Takacs, L. L., 1985: A two-step scheme for the advection equation with minimized dissipation and dispersion errors. *Mon. Wea. Rev.,* **113**, 1050–1065.

Young, D. M., and R. T. Gregory, 1972: *A Survey of Numerical Mathematics,* Vol. I. Addison-Wesley, 492 pp.